JOURNAL OF CHEMICAL INFORMATION AND MODELING

Article

pubs.acs.org/jcim

CHARMM-GUI Micelle Builder for Pure/Mixed Micelle and Protein/Micelle Complex Systems

Xi Cheng,[†] Sunhwan Jo,[†] Hui Sun Lee,[†] Jeffery B. Klauda,[§] and Wonpil Im*[,†]

[†]Department of Molecular Biosciences and Center for Bioinformatics, The University of Kansas, 2030 Becker Drive, Lawrence, Kansas 66047, United States

[§]Department of Chemical and Biomolecular Engineering, The University of Maryland, 2113 Chemical and Nuclear Engineering, College Park, Maryland 20742, United States

Supporting Information

ABSTRACT: *Micelle Builder* in CHARMM-GUI, http://www.charmm-gui.org/input/micelle, is a web-based graphical user interface to build pure/mixed micelle and protein/micelle complex systems for molecular dynamics (MD) simulation. The robustness of *Micelle Builder* is tested by simulating four detergent-only homogeneous micelles of DHPC (dihexanoylphosphatidylcholine), DPC (dodecylphosphocholine), TPC (tetradecylphosphocholine), and SDS (sodium dodecyl sulfate) and comparing the calculated micelle properties with experiments and previous simulations. As a representative protein/micelle model, Pf1 coat protein is modeled and simulated in DHPC micelles with three different numbers of DHPC molecules. While the number of DHPC molecules in direct contact with Pf1 protein converges during the simulation, distinct behavior and geometry of micelles lead to different protein conformations in comparison to that in bilayers. It is our hope that CHARMM-GUI *Micelle Builder* can be used for simulation studies of various protein/micelle systems to better understand the protein structure and dynamics in micelles as well as distribution of detergents and their dynamics around proteins.

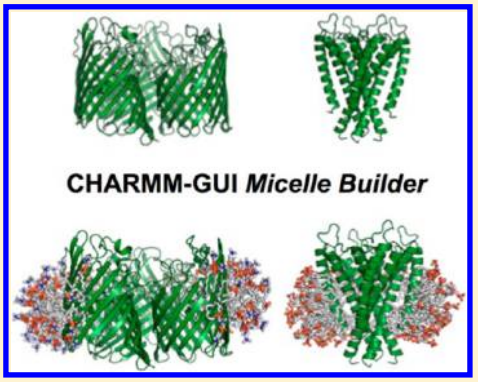

INTRODUCTION

Micelles are frequently used in biochemical studies as a mimetic of cell membranes to solubilize integral membrane proteins.[1−3] Understanding the effects of micelles on membrane proteins is significant in determining optimal detergent conditions for extraction, purification, and characterization of proteins.[3−5] As a result, studying membrane proteins in micelles with atomic resolution has been of great interest to experimental and computational biophysicists.[6−21] Molecular dynamics (MD) simulation is an attractive approach to study such systems because simulation can provide information about the structures, dynamics, interactions, and energetics of micelle systems at the atomic level, which is generally hard to obtain solely from experiments.

It is well-known that detergents in water can readily self-assemble to form micelles. Nonetheless, with few exceptions for small detergent aggregations,[22] self-assembly simulation requires long relaxation time and a large amount of water and detergent molecules, which are computationally expensive. Recently, Pires et al. performed a 1 μs coarse-grained MD simulation to characterize the sodium dodecyl sulfate (SDS) micelle formation.[6] 360 SDS and 90,000 water particles were included in the micelle system, whose relaxation occurred after about 250 ns. For the study of protein in micelles, Böckmann and Caflisch simulated spontaneous micelle formation of 1,2-dihexanoyl-*sn*-glycero-phosphocholine (DHPC) around OmpX, which included 125−188 detergents and required ∼40 ns for equilibration.[7] To avoid long relaxation times and large systems, most computational studies are conducted on preassembled models.[8,16−18] However, building a preassembled protein/micelle complex is still challenging and requires considerable experience with simulation software. The main difficulty in building such a complex system arises from how to distribute detergents around a protein, especially when the protein is an irregular shape, although detergents adjust themselves in concert with the embedded protein in the course of MD simulations.[7,8]

Currently, there are several websites and programs, e.g., CHARMM-GUI,[23−25] CHARMMing,[26] and InflateGRO2,[27] that support users to build complex protein or protein−lipid systems for MD simulations. Much effort has been made on building lipid bilayers and proteins that exist in these bilayers, but there lacks any website or program to build lipid micelles that are commonly used to study membrane proteins. To simplify and automate the building process of protein/micelle preassembled complex systems for MD simulations, we have developed *Micelle Builder* (http://www.charmm-gui.org/input/micelle), a graphical user interface (GUI) available at the CHARMM-GUI website.[25] Using *Micelle Builder*, a user can

Received: May 6, 2013
Published: July 18, 2013

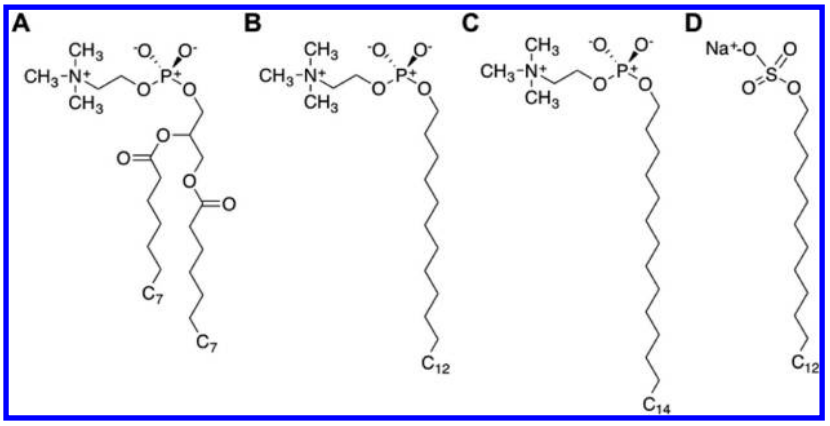

Figure 1. Chemical structures of (A) DHPC, (B) DPC, (C) TPC, and (D) SDS.

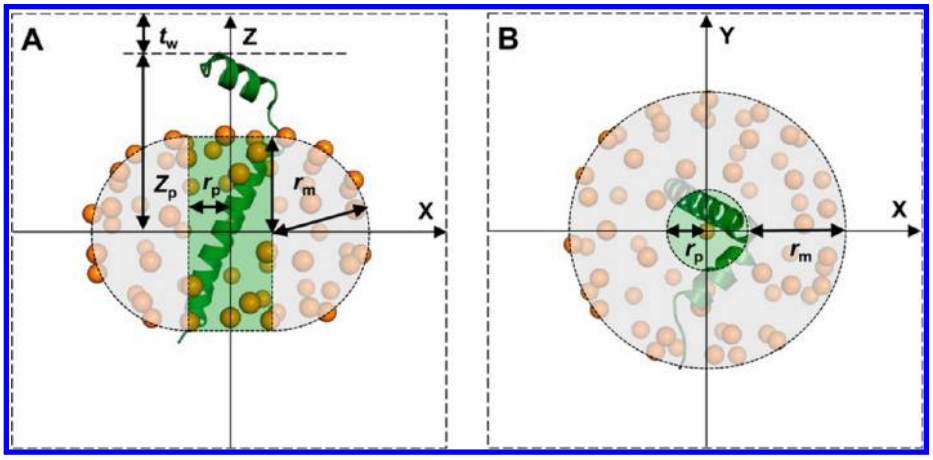

Figure 2. Schematic representation of a Pf1 coat protein/micelle system: (A) side and (B) top views. The protein/micelle complex size on *XY* plane (L_{XY}) is twice the sum of protein radius (r_p) and micelle radius (r_m), i.e., $L_{XY} = 2r_m + 2r_p$. The complex size along the *Z* axis (L_Z) is twice the larger one between the maximum absolute Z coordinate of the protein ($\max(|Z_p|)$) and r_m. The system size is the larger one of L_{XY} and L_Z plus twice the water thickness (t_w). The protein is shown in green cartoon representation, and the headgroup phosphorus atoms are shown in orange sphere. The green area indicates a protein hydrophobic region. Together with the green one, the light gray area represents the initial detergent-distributed region.

upload a membrane protein structure or download from a database and choose one or multiple detergent types to generate a preassembled micelle around the protein. The complicated building process of protein/micelle systems can be dramatically simplified by automating the process with the intuitive user interface. In addition to the protein/micelle system, a user can also generate a detergent-only system without protein. All the necessary input files for building the system are provided to users, so that more complex modeling or adaptation of the protocol is possible, if necessary.

In this paper, we describe and illustrate the standardized building process of micelle and protein/micelle complex systems in CHARMM-GUI *Micelle Builder*. For illustration, we simulated four representative homogeneous micelle systems composed of DHPC, *n*-dodecylphosphocholine (DPC or FC-12), *n*-tetradecylphosphocholine (TPC or FC-14), and SDS, respectively (Figure 1). The resulting models were compared with experimental data and previous simulation studies. In addition, we also used *Micelle Builder* to build and simulate the major coat protein of bacteriophage Pf1 (Pf1 protein hereinafter) in three micelles with 50, 75, and 100 DHPC molecules. The Pf1 protein is composed of a C-terminal single-pass transmembrane helix and a N-terminal periplasmic helix. Its structure was recently determined based on both solid-state and solution NMR observables, assuming that the protein structure is highly similar in bilayers and in micelles.[28] On the basis of these simulations, we explored the differences between protein-detergent interactions in micelles and protein−lipid interactions in bilayers.

METHODS

Protein/Micelle Complex Building Process in CHARMM-GUI *Micelle Builder*. The overall process to build a protein/micelle complex simulation system has been generalized and automated in six steps (Supporting Information Figure S1), similar to *Membrane (Bilayer) Builder*[29,30] in the CHARMM-GUI website, http://www.charmm-gui.org.[25] Each step is designed to incorporate user-specified parameters through a web browser and generate/execute CHARMM input files. The user can download and check the generated system in each step so that, if necessary, one can go back to the previous step and modify the options interactively. For a detergent-only micelle, the building procedure starts from the size-determination *STEP 3* (Figure S1). Individual input and output files or archives of all files are available for download.

STEP 1: Read Protein Structure. The building process of a protein/micelle system starts with reading a protein structure into CHARMM. Users can upload their own protein structure or specify a Protein Data Bank (PDB)[31] entry ID and a database to download the PDB file. Protein structures from the

OPM (Orientations of Proteins in Membranes) database,[32] http://opm.phar.umich.edu, are preoriented with respect to the membrane normal (the Z axis by definition). Like *Membrane (Bilayer) Builder*, the usage of OPM database is recommended over the PDB[33] in *Micelle Builder* (see below).

STEP 2: Orient Protein. *Micelle Builder* assumes that the initial protein structure is oriented along the Z axis and the hydrophobic region of the protein is placed around $Z = 0$, which is the same as in *Membrane (Bilayer) Builder*. In the case that the protein is not properly oriented along the Z axis, *Micelle Builder* provides a few options so that the user can place the protein appropriately in a micelle by reorienting the protein. These options are as follows: aligning the protein principal axis along the Z axis; aligning a vector between two user-specified Cα atoms along the Z axis; translating the protein along the Z axis; and rotating the protein around the X axis. After alignment, *Micelle Builder* generates pore water,[24] if specified, and calculates the protein cross-sectional area along the Z axis, which provides information on the protein position with respect to the Z axis (Figure S2).

STEP 3: Determine System Size. This is a critical step to determine the system size, based on a number of user-specified parameters such as detergent type, number of detergents, water thickness around the micelle, and the size of the protein's hydrophobic region (Figure 2). In the current *Micelle Builder* setup, a cubic box is assumed for a micelle system, and four detergent molecules (DHPC, DPC, SDS, and TPC; Figure 1) are available. A user needs to select one or more detergent types and specify the number of selected detergent type(s) in the table under "Number of Detergent Molecules". The detergent number per micelle generally needs to be equal or larger than the aggregation number of homogeneous micelle, i.e., 35 (DHPC),[9] 54 (DPC),[11] 108 (TPC),[10] and 62 (SDS).[12] This information is provided next to "Number of Detergent Molecules". For homogeneous micelles, an initial micelle radius (r_m) is set to 21.4 Å (DHPC), 21.4 Å (DPC), 26.9 Å (TPC), and 22.6 Å (SDS) based on the pure micelle simulations in this study. As shown in Figure 2, the protein hydrophobic region (green area) is defined by its heavy atoms' Z coordinates (Z_p) ranging from $-r_m$ to r_m. The protein radius (r_p) on the XY plane is set to the larger one between the average radius of hydrophobic region heavy atoms on XY and the average radius of hydrophobic region heavy atoms in -2.5 Å $< Z <$ 2.5 Å on XY. Using this metric helps place detergent molecules for proteins with various geometries (see below). Then, the protein/micelle complex size on the XY plane (L_{XY}) is set to $2r_m + 2r_p$. If the protein is completely buried in the micelle, i.e., $\max(|Z_p|)$ is less than r_m, then the complex size along the Z axis (L_Z) is set to $2r_m$. Otherwise, $L_Z = 2\max(|Z_p|)$. The system size is the larger one of L_{XY} and L_Z plus twice the water thickness (t_w) from the complex.

After the system size is determined, *Micelle Builder* provides a detailed summary of the system size as well as a model micelle system with detergent-like pseudoatoms in the headgroup region (step3_packing.pdb). This model protein/micelle system can provide an idea about the initial detergent distribution, i.e., the detergent packing around the protein, because the pseudoatom positions are used to place detergent molecules in *STEP 4*. Briefly, a single-type pseudoatom with a radius of 5.4 Å is used to approximate the head groups of different detergents. Initially, each pseudoatom (for selected detergents) is randomly distributed on a torus surface (surface of green and light gray regions in Figure 2) but not inside protein pores (if a protein has a pore) via Monte Carlo simulations using a primitive model, i.e., van der Waals and 80-scaled Coulombic interactions. It is important for a user to visually examine the system packing with the resulting structure file (step3_packing.pdb) because it is generally not known how many detergent molecules should be around a protein experimentally. Therefore, if the number of detergent molecules appears to be smaller or larger than expected, the user needs to go back to the previous step and adjust parameters.

STEP 4: Build Components. In this step, the system components such as a detergent micelle, bulk water, and ions are generated. The detergent micelle is built by a replacement method using the positions of detergent-like pseudoatoms in the headgroup region, determined in *STEP 3* (step3_packing.pdb). Each pseudoatom is sequentially selected, and its coordinate is used to place the headgroup of a randomly selected detergent molecule from the corresponding detergent structural library. A structural library of 2000 different conformations for each detergent type was generated from the homogeneous micelle simulations in this study. With the headgroup sulfur/phosphorus atom position fixed, each detergent molecule is reoriented to ensure its carbon tail placed within the micelle hydrophobic core around the protein. To make the system neutral, *Micelle Builder* generates an appropriate number of ions, depending on the user-specified ion concentration. The initial configuration of ions is then determined around the generated protein/micelle complex via Monte Carlo simulations using the primitive model used in *STEP 3*.

STEP 5 and 6: Assemble Components and Equilibrate the System. Each component generated in the previous step is assembled in *STEP 5*. The user needs to examine the assembled system (step5_assembly.pdb) and verify whether the system has been built as intended. Because of the significant computing resources required for system equilibration, *Micelle Builder* does not provide the equilibrated structure. Instead, *Micelle Builder* provides the six consecutive CHARMM[34] and NAMD[35] input files for system equilibration and the simulation production inputs. As shown in Table S1, to ensure gradual equilibration of the uncorrelated initial system, harmonic restraints are applied to the ions, heavy and side chain atoms of protein, and detergent sulfur/phosphorus atoms. These restraint forces are slowly reduced as the equilibration processes.

Detergent-Only Homogeneous Micelle Systems. To illustrate the robustness of *Micelle Builder*, we constructed and simulated detergent-only homogeneous micelle systems (Table 1 and Figure 3) for four commonly used detergents: DHPC, DPC, TPC, and SDS. According to previous experimental and computational studies, we used 35 DHPC,[9] 54 DPC,[11] 108 TPC,[10] and 62 SDS[12] molecules to characterize corresponding

Table 1. System Information

system name	# detergents	# water	# ions	# total atoms
DHPC	35	11,250	20 K^+, 20 Cl^-	36,450
DPC	54	11,988	23 K^+, 23 Cl^-	39,304
TPC	108	17,505	38 K^+, 38 Cl^-	59,827
SDS	62	13,845	71 Na^+, 9 Cl^-	44,219
Pf1-DHPC50	50	13,242	43 K^+, 42 Cl^-	44,276
Pf1-DHPC75	75	19,236	62 K^+, 61 Cl^-	64,196
Pf1-DHPC100	100	26,872	85 K^+, 84 Cl^-	89,051

dx.doi.org/10.1021/ci4002684 | J. Chem. Inf. Model. 2013, 53, 2171−2180

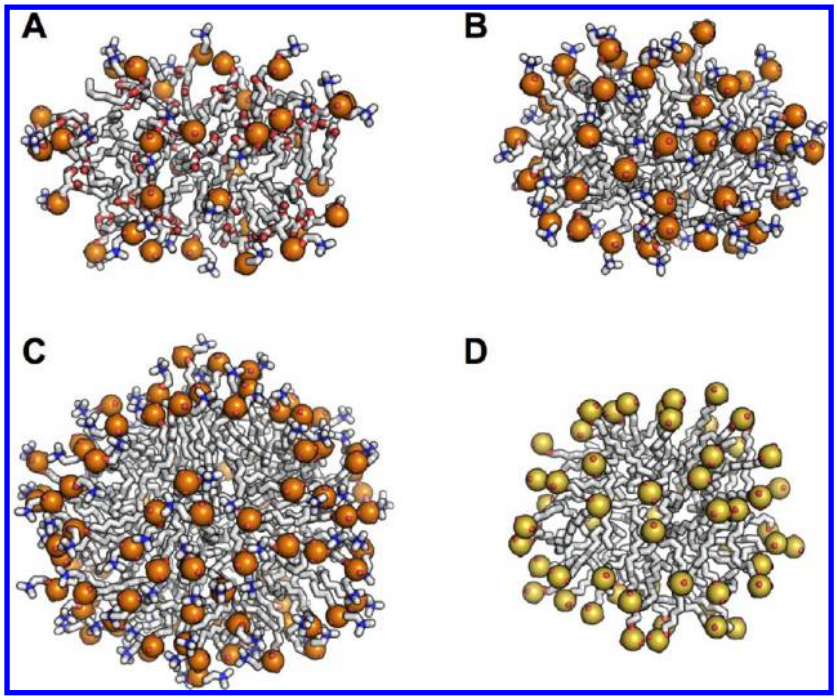

Figure 3. Representative structures of (A) DHPC, (B) DPC, (C) TPC, and (D) SDS micelles. Water and ions are omitted for clarity. The headgroup phosphorus (orange)/sulfur (yellow) atoms are shown in spheres and others in stick models.

Table 2. Geometrical Parameters[a] of Detergent Micelles

detergent	r_m (Å)	R_g (Å)	r_m[b] (Å)	R_g[c] (Å)	I_{max}/I_{min}	<S> (Å^2)
DHPC	21.4 ± 0.2	16.8 ± 0.2	NR[d]	NR[d]	1.57 ± 0.11	338.9 ± 6.3
DPC	21.4 ± 0.1	16.5 ± 0.1	22.2[13]	17.4[16]	1.22 ± 0.04	218.8 ± 3.5
			19.5−24.5[15]			
			21−22[16]			
TPC	26.9 ± 0.1	21.0 ± 0.1	NR[d]	NR[d]	1.27 ± 0.05	181.4 ± 2.6
SDS	22.6 ± 0.1	15.1 ± 0.1	22.8[13]	15.5 ± 0.1[19]	1.31 ± 0.06	174.9 ± 2.5
			22.3[14]	15.7 ± 0.2[17]		

[a]Calculated values are the mean ± standard errors over the 5 independent simulation systems. [b]Micelle radius (r_m) was taken from the literature. [c]Micelle radius of gyration was taken from the literature. [d]NR, no reference was available.

homogeneous micelle properties. The micelle-only generation option in *Micelle Builder* was used to build these four systems. 0.15 M KCl was used for DHPC, DPC, and TPC systems, while 0.15 M NaCl was used for SDS to match experiments.[12−14] The molecular force field of these detergent molecules are based on the CHARMM36 (C36) lipid force field,[36] and a TIP3P water model[37] was used. Each system was replicated and assigned with different velocities to generate five independent simulation systems, resulting in a total of 20 simulation systems. All calculations were performed in NPT (constant particle number, pressure, and temperature) ensembles[38] at 303.15 K using NAMD 2.8,[35] a parallel code designed for high-performance simulation of large biological macromolecule using the CHARMM force field.[34,36,39] The particle mesh Ewald algorithm[40] was applied to calculate electrostatic forces, and the van der Waals interactions were smoothly switched off at 10−12 Å by a force-switching function.[41] A time step of 2 fs was used in all simulations. After equilibration, a 100-ns production run was performed for each system. All average micelle properties were calculated over the five replicas using the last 40-ns simulations and presented with standard errors (Table 2).

Pf1 Protein/Micelle System. The average NMR structure of Pf1 protein (PDB:2KSJ) was chosen as the starting protein structure. The protein structure was determined using a hybrid method combining solution NMR observables obtained from DHPC micelles and solid-state NMR observables from bilayers. Since the aggregation number of DHPC around Pf1 protein is not known, we used three different aggregation numbers (50, 75, and 100 DHPC molecules) to distribute DHPC molecules around the protein surface to mimic the NMR experimental conditions.[28] The protein/micelle generation option in *Micelle Builder* was used to build these systems including 0.15 M KCl (Table 1 and Figure 4). Each system was replicated and assigned with different velocities to generate three independent simulation systems. All calculations were performed in NPT ensembles at 303.15 K using NAMD 2.8[35] and the CHARMM force field.[34,36,39] A time step of 2 fs was used, and a 100-ns production run was performed for each system.

RESULTS AND DISCUSSION

Micelle Size and Shape. The most characteristic measurement of the micelle size is its radius. As shown in Figure S3, the micelle radius (r_m) is defined as the average distance (r_h) of the headgroup sulfur/phosphorus atoms from the micelle's center

dx.doi.org/10.1021/ci4002684 | J. Chem. Inf. Model. 2013, 53, 2171−2180

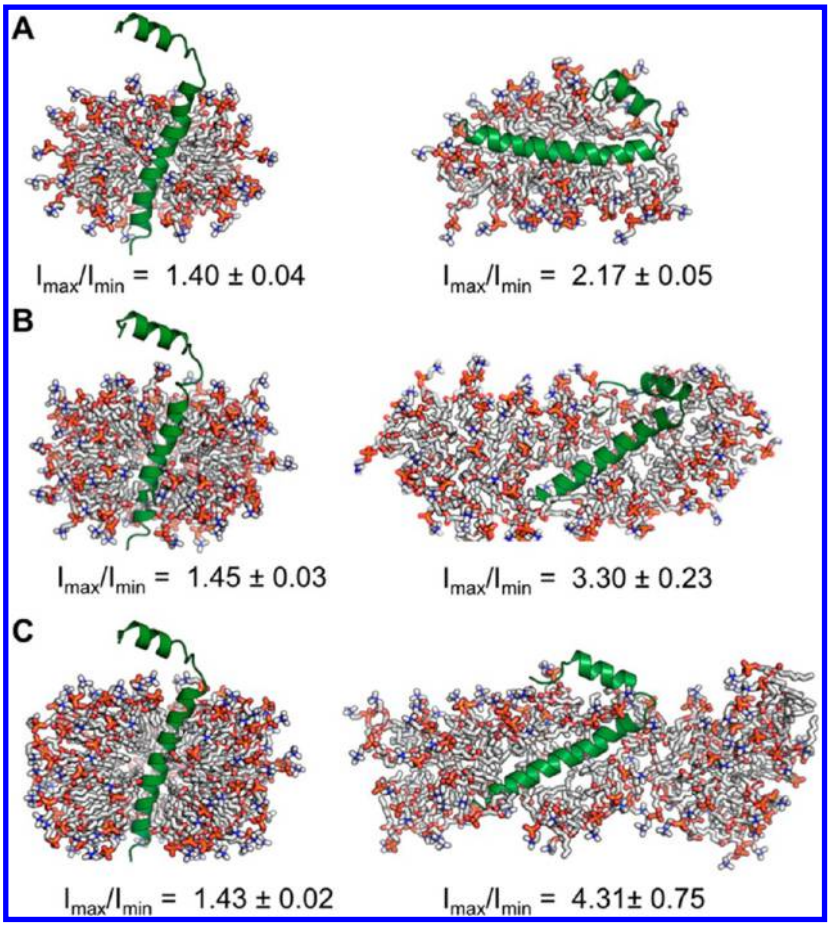

Figure 4. Initial (left) and equilibrated (right) structures of Pf1 coat protein in the DHPC micelles with (A) 50, (B) 75, and (C) 100 aggregation numbers. The ratio between maximum and minimum moment of inertia (I_{max}/I_{min}) for the initial (first 2 ns) and equilibrated (last 2 ns) structures are listed below the corresponding system snapshots. The protein is presented in green and the detergents are shown with sticks. Ions, water, and detergents blocking the view of the protein are omitted for clarity.

of mass (COM) plus the distance (d) at the first peak of the sulfur/phosphorus to water oxygen radial distribution function minus the radius of water (r_w = 1.4 Å); i.e., $r_m = r_h + d - r_w$.[18] This definition represents an effective micelle radius. In addition, the micelle radius of gyration was calculated by

$$R_g = \sqrt{\frac{1}{N}\sum_{i=1}^{N}(|\mathbf{r}_i| - \langle r\rangle)^2} \quad (1)$$

where $\langle r\rangle$ is the mean distance of the heavy atoms ($\mathbf{r}_i$) from the micelle COM (centered at the origin). R_g are stable as a function of time in all systems (Figure S4), indicating the convergence of the system, although less than three detergents dissociates from the micelles in a few simulation systems. As shown in Table 2, the average values of r_m and R_g in this work quantitatively agree with those observed in the previous experiments[13−15] and simulations,[6,16,17] demonstrating the robustness of our models and simulation set up in *Micelle Builder*.

The shape and stability of a micelle can be characterized by its moment of inertia (I) along the X, Y, or Z axis, defined by

$$I = \sum_{i=1}^{N} m_i r_i^2 \quad (2)$$

where m_i is the mass of an atom i, and r_i is the distance of the atom from the axis. I_{max}/I_{min} is the ratio between the largest moment of inertia and the smallest one. For a perfect sphere, I_{max}/I_{min} = 1. As shown in Table 2, none of these micelles are perfectly spherical. The average values of I_{max}/I_{min} in DPC and SDS are 1.22 and 1.31, which are in the range reported for previous DPC simulations (1.2[8]−1.24[16]) and SDS simulations (1.05[18]−1.39[17]). Compared to the other micelles, DHPC is least spherical (I_{max}/I_{min} = 1.57) and such a prolate shape was also observed by small-angle X-ray scattering.[42]

Micelle Structure. Micelle structure can be analyzed in terms of radial densities of different components from the micelle COM (Figure 5). The shapes of the density distributions are in good agreement with those of previous simulations.[8,17,19] The interior of micelle is void of solvent, as observed in experiments[20,21] and other simulations.[8,17,19] The solvent-detergent interface, i.e., the overlapping area of detergent carbon tail and water distributions in Figure 5, is broader in DHPC micelles due to its nonspherical nature described in the previous section. In SDS systems, some sodium ions stay close to the micelle surface because of electrostatic interactions with negatively charged SDS head groups, while potassium ions do not associate with the micelle in the other systems. As an additional analysis to characterize the micelle structural properties, the accessible molecular surface area (SA) was calculated as follows; all of the ions and water molecules were removed from the system, a probe molecule with a radius of 1.4 Å was rolled over the surface of

dx.doi.org/10.1021/ci4002684 | J. Chem. Inf. Model. 2013, 53, 2171−2180

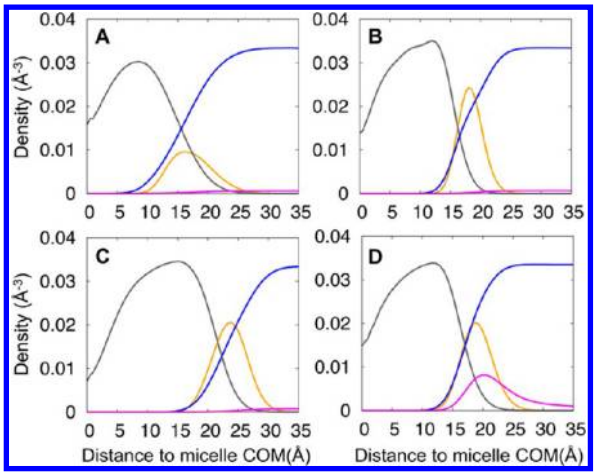

Figure 5. Density profiles for the specific components from the micelle center of mass: micelle carbon tails (*gray*), head groups (*orange*), water (*blue*), and positive ions (*magenta*) in (A) DHPC, (B) DPC, (C) TPC, and (D) SDS micelles. These plots are produced by counting the number of selected atoms that are within 0.5 Å shells along the radial distance from the micelle center of mass. The density values of micelle head groups and positive ions are multiplied by 10 for clarity.

the micelle, and then the contact area was summed to quantify the total *SA*. The accessible surface area per detergent (<*S*>) calculated by dividing the total *SA* by the number of detergents in each system is listed in Table 2. Bruce et al.[18] reported a value of 176 Å^2 for SDS micelles, which is quite similar to our calculated value (174.9 ± 2.5 Å^2).

Distribution and Mobility of Detergents in Protein/Micelle Systems. In addition to the Pf1 protein/micelle systems in Figure 4, we have built various protein/micelle complex structures to examine/validate the robustness of the building process in *Micelle Builder*. As shown in Figure 6A–C, *Micelle Builder* is able to build the protein/micelle initial models for various topologies of α-helical membrane proteins,[43,44] even for the conical shape of KcsA K^+ channel tetramer.[45] As shown in Figure 6D-E, β-barrel proteins such as OmpA[46] and OmpF[47] can be well solvated in micelles through *Micelle Builder*. In the case of OmpF, the option for generating pore water molecules in *STEP 2* was used to properly solvate the barrel interior. These initial structures can be relaxed with the rearrangement of detergent molecules in the course of simulation, as illustrated with our recent simulation studies[48] of DAP12-NKG2C (Figure 6B) as well as Pf1 in the following paragraph.

As a representative model, the Pf1 protein/micelle complex systems with different DHPC aggregation numbers (50, 75, and 100) are further characterized with the 100-ns simulations (Figure 4). Interestingly, even though the total number of detergents varies in the different systems (depending on its initial aggregation number), the number of detergents in direct contact with the protein becomes very similar within 10 ns (Figure 7A-B): 36 ± 3 for Pf1/DHPC50, 38 ± 3 for Pf1/DHPC75, and 38 ± 4 for Pf1/DHPC100. Clearly, the torus of initial detergent molecules around the Pf1 adjusts its shape in concert with Pf1 and adapts less spherical geometry as more detergents involved in the complex during the simulation (Figure 4). In this process of redistribution, some detergents dissociate from the complex and come back afterward (Figure 7C-E). Compared to Pf1-DHPC50, Pf1-DHPC75 and Pf1-DHPC100 have larger numbers of dissociating detergents (Figure 7B and S5). Even with this variation, the current 100-ns simulations do not provide any information of possible aggregation numbers of DHPC around Pf1. Nonetheless, the simulations do provide a good estimation of the Pf1-contact detergent number and demonstrate that the smallest system of 50 DHPC is sufficient to solvate Pf1 protein. Therefore, we will focus on this Pf1-DHPC50 system for further analysis.

Protein-Detergents Interactions and Its Effect on Protein Structure. The previous bilayer simulations of Pf1 protein show that protein–lipid interactions affect the

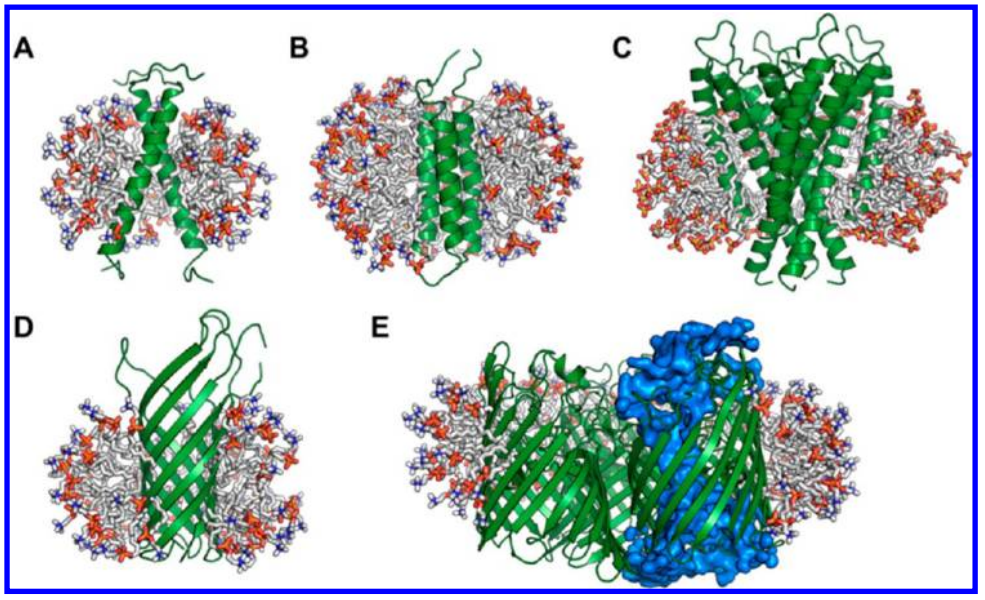

Figure 6. Protein/micelle complex structures for (A) GpA (PDB:1AFO)[39] with 55 DPC molecules, (B) DAP12-NKG2C (PDB:2L35)[38] with 13 SDS and 130 TPC molecules, (C) KcsA tetramer (PDB:1R3J)[45] with 180 SDS molecules, (D) OmpA (PDB:1BXW)[46] with 80 DPC molecules, and (E) OmpF trimer (PDB:3POX)[47] with 160 DPC molecules. The protein is presented in green, the detergents are shown as gray sticks, and pore water in one monomer of OmpF is shown in blue surface representation. Ions, water, and detergents blocking the view of the protein are omitted for clarity.

dx.doi.org/10.1021/ci4002684 | *J. Chem. Inf. Model.* 2013, 53, 2171–2180

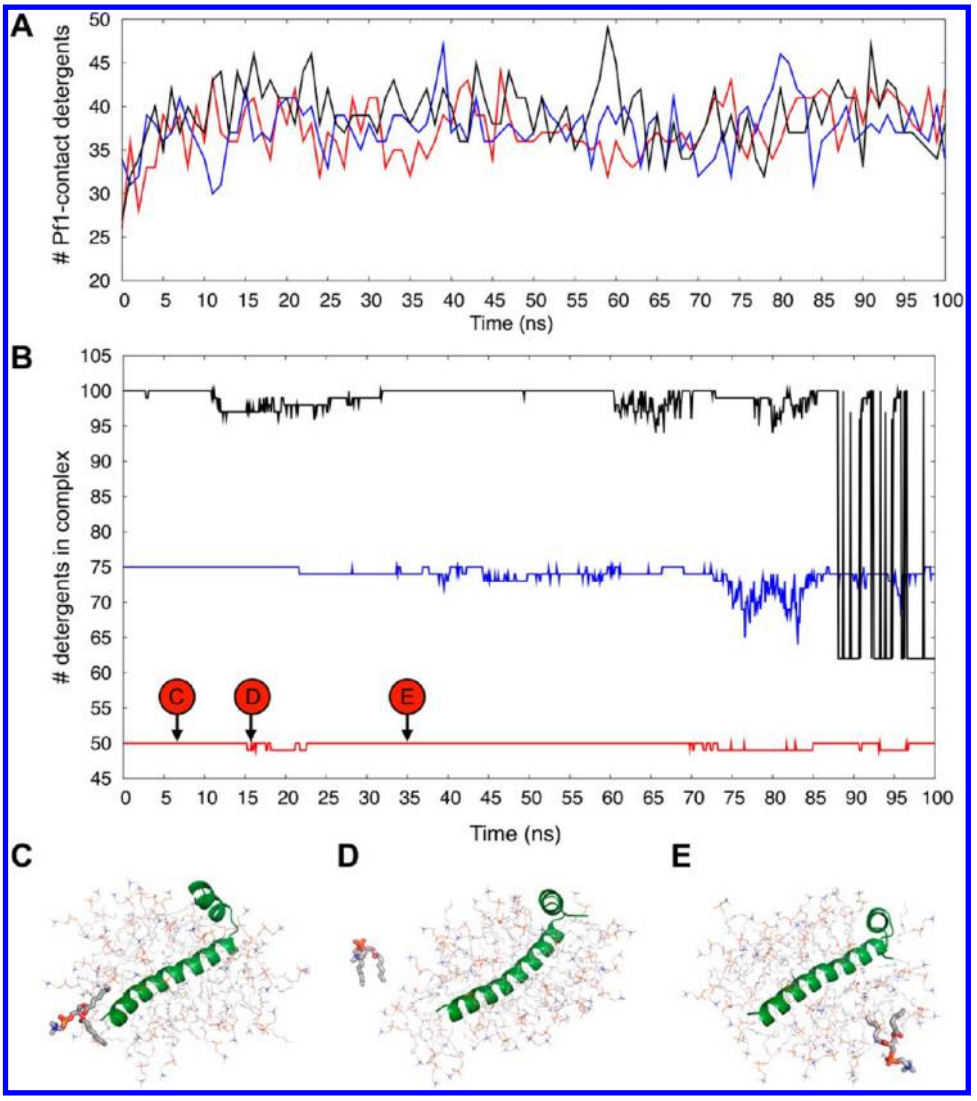

Figure 7. (A) The number of Pf1-contact detergents as a function of time in Pf1-DHPC50 (*red*), Pf1-DHPC75 (*blue*), and Pf1-DHPC100 (*black*) systems. A detergent is counted as a contact detergent when any of its heavy atoms is within 4 Å from the Pf1 protein heavy atoms. (B) The number of detergents in the protein/micelle complex as a function of time in Pf1-DHPC50 (*red*), Pf1-DHPC75 (*blue*), and Pf1-DHPC100 (*black*) systems. A detergent is counted as a complex detergent when a detergent is in contact (within 4 Å) with the protein or the detergents embedding the protein. In Pf1-DHPC50, three snapshots were taken at (C) 7 ns, (D) 16 ns, and (E) 35 ns to show the dynamic behavior of one detergent molecule leaving and coming back to the complex. The protein is presented in green, the detergents are shown as gray lines, and the dissociating detergents are in stick models. Ions, water, and detergents blocking the view of the protein are omitted for clarity.

orientation of the periplasmic helix (Figure 8), especially the hydrophobic interactions involving residues A7, V8, A11, and I12 in the periplasmic helix.[49] In the micelle simulations, protein−solvent interacting patterns are quite similar to those in bilayers (Figure 8). However, more frequent and specific hydrophobic interactions between hydrophobic residues (A7, V8, A11, and I12) in the periplasmic helix and detergents were observed in the micelles compared to those between the residues and lipids in the bilayer system (Figure 9).

The Pf1 coat protein consists of two helices. Both transmembrane and periplasmic helices have root-mean-squared deviation (RMSD) from the average NMR structure (PDB:2KSJ) around 1 Å during the Pf1-DHPC50 simulations. However, as observed in the previous experiments[28] and bilayer simulations,[49] the periplasmic helix orientation is highly flexible (Figure 10), which contributes to large overall RMSD of 7.3 ± 1.7 Å in Pf1-DHPC50. As mentioned above, the interactions between the periplasmic helix and detergents/lipids contribute to its orientation. Considering this important association as well as the distinctive geometries between micelle and bilayer, Pf1 protein (with the periplasmic helix) may present different conformations in the different environments (Figure S6). In terms of the angle between the transmembrane and periplasmic helices, Pf1 protein essentially has no angle smaller than 60° in the bilayers, while it has a large population with angles 20−60° in the micelles (Figure 10). Our simulation results suggest that, while micelles are effective mimetic for membrane bilayers and could hold the membrane protein's individual structural components as well as transmembrane domain,[48] they may not well-maintain orientations between the transmembrane domain and other structural elements existing on the outside or periphery of membrane bilayers.

■ CONCLUSIONS

We have described the generalized and automated procedure to build a protein/micelle complex system for MD simulation

dx.doi.org/10.1021/ci4002684 | J. Chem. Inf. Model. 2013, 53, 2171−2180

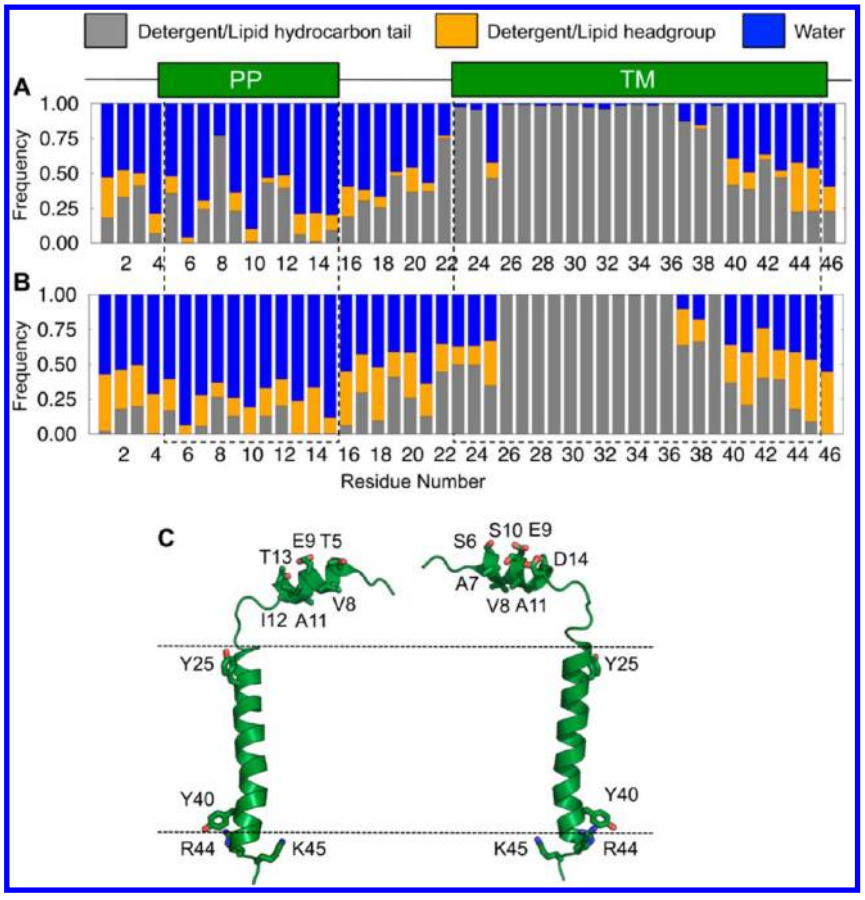

Figure 8. Interactions between Pf1 residues and various components in (A) Pf1-DHPC50 (micelle) and (B) Pf1-DOPC/DOPG (bilayer)[49] systems. The graph shows the frequency with which any heavy atom of each residue is found within 4 Å of detergent or lipid carbon tails, detergent or lipid head groups, and water. The green rectangles indicate transmembrane (TM) and periplasmic (PP) helical residues. (C) Residues important for stabilizing TM and PP helix orientations relative to the membrane.

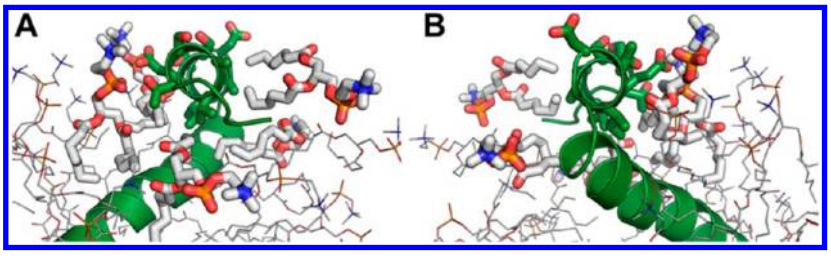

Figure 9. Snapshots showing the interactions between Pf1 coat protein periplasmic helix and detergent molecules in (A) front and (B) back views. The protein is shown in green. Residues in the periplasmic helix are shown as sticks. Detergents are shown as gray lines; those contacting with the periplasmic helix are drawn as sticks. Water molecules and detergents blocking the views of protein are omitted for clarity.

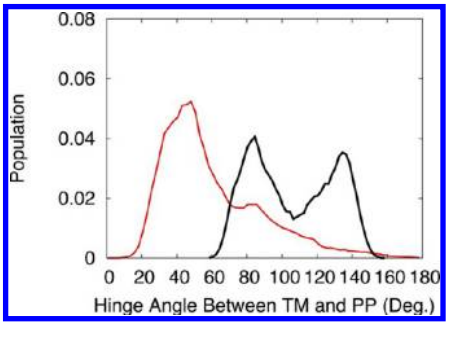

Figure 10. Distribution of angles between the transmembrane (TM) and periplasmic (PP) helices of Pf1 protein in the DHPC micelle (*red*) and DOPC/DOPG bilayer[49] (*black*).

using *Micelle Builder* in CHARMM-GUI. Its robustness was first tested by building and simulating four representative homogeneous micelle systems of DHPC, DPC, TPC, and SDS. During the simulations, all micelle systems were stable. The size, shape, and structure of resulting micelles are in quantitative agreement with available experimental data and other simulation studies.

Instead of using a spherical model, the torus-shaped micelle building method in *Micelle Builder* was developed to generate protein/micelle complex structures. As illustrated with distinct topologies of α-helical and β-barrel membrane proteins, this method can be applied to various proteins with different geometries. As a representative, Pf1 protein/micelle systems were built, simulated, and characterized. Due to the larger mobility of detergents in a micelle, the detergents can interact

dx.doi.org/10.1021/ci4002684 | J. Chem. Inf. Model. 2013, 53, 2171−2180

with specific sites on the protein where their lipid counterparts may not due to bilayer's (planar) geometric restriction. In the Pf1 case, the different geometries of micelle and bilayer appear to affect the structure and orientation of a protein domain outside or at the periphery of the membrane and thus lead to different overall protein structures. It is our hope that CHARMM-GUI *Micelle Builder* is used for simulation studies of various protein/micelle systems to better understand the protein structure and dynamics in micelles as well as distribution of detergents and their dynamics around protein.

■ ASSOCIATED CONTENT

Supporting Information

Force constants for positional harmonic restraints on each equilibration step (Table S1). Overview of building process of protein/micelle complex simulation systems in CHARMM-GUI *Micelle Builder* (Figure S1). Cross-sectional area profile of Pf1 coat protein generated by *Micelle Builder* (Figure S2). Schematic representation of the micelle radius (Figure S3). Micelle radius of gyration as a function of time in DHPC, DPC, TPC, and SDS (Figure S4). Two snapshots in Pf1-DHPC100 (Figure S5). Snapshots of Pf1 protein in bilayer and micelle systems (Figure S6). This material is available free of charge via the Internet at http://pubs.acs.org.

■ AUTHOR INFORMATION

Corresponding Author

*E-mail: wonpil@ku.edu.

Notes

The authors declare no competing financial interest.

■ ACKNOWLEDGMENTS

This work was supported in part by NSF MCB-1157677, NSF ABI-1145987, and XSEDE resources (TG-MCB070009).

■ REFERENCES

(1) Columbus, L.; Lipfert, J.; Klock, H.; Millett, I.; Doniach, S.; Lesley, S. A. Expression, purification, and characterization of Thermotoga maritima membrane proteins for structure determination. *Protein Sci.* **2006**, *15*, 961−975.

(2) Eshaghi, S.; Hedren, M.; Nasser, M. I.; Hammarberg, T.; Thornell, A.; Nordlund, P. An efficient strategy for high-throughput expression screening of recombinant integral membrane proteins. *Protein Sci.* **2005**, *14*, 676−683.

(3) Sanders, C. R.; Sonnichsen, F. Solution NMR of membrane proteins: practice and challenges. *Magn. Reson. Chem.* **2006**, *44 Spec No*, S24−40.

(4) Berger, B. W.; Garcia, R. Y.; Lenhoff, A. M.; Kaler, E. W.; Robinson, C. R. Relating surfactant properties to activity and solubilization of the human adenosine a3 receptor. *Biophys. J.* **2005**, *89*, 452−464.

(5) Wiener, M. C. A pedestrian guide to membrane protein crystallization. *Methods* **2004**, *34*, 364−372.

(6) Pires, J. M.; de Moura, A. F.; Freitas, L. C. G. Investigating the spontaneous formation of sds micelle in aqueous solution using a coarse-grained force field. *Quim. Nova* **2012**, *35*, 978−981.

(7) Bockmann, R. A.; Caflisch, A. Spontaneous formation of detergent micelles around the outer membrane protein OmpX. *Biophys. J.* **2005**, *88*, 3191−3204.

(8) Bond, P. J.; Sansom, M. S. P. Membrane protein dynamics versus environment: Simulations of OmpA in a micelle and in a bilayer. *J. Mol. Biol.* **2003**, *329*, 1035−1053.

(9) Columbus, L.; Lipfert, J.; Jambunathan, K.; Fox, D. A.; Sim, A. Y.; Doniach, S.; Lesley, S. A. Mixing and matching detergents for membrane protein NMR structure determination. *J. Am. Chem. Soc.* **2009**, *131*, 7320−7326.

(10) Strop, P.; Brunger, A. T. Refractive index-based determination of detergent concentration and its application to the study of membrane proteins. *Protein Sci.* **2005**, *14*, 2207−2211.

(11) Tieleman, D. P.; van der Spoel, D.; Berendsen, H. J. C. Molecular dynamics simulations of dodecylphosphocholine micelles at three different aggregate sizes: Micellar structure and chain relaxation. *J. Phys. Chem. B* **2000**, *104*, 6380−6388.

(12) Turro, N. J.; Yekta, A. Luminescent probes for detergent solutions - simple procedure for determination of mean aggregation number of micelles. *J. Am. Chem. Soc.* **1978**, *100*, 5951−5952.

(13) Gao, X.; Wong, T. C. Studies of the binding and structure of adrenocorticotropin peptides in membrane mimics by NMR spectroscopy and pulsed-field gradient diffusion. *Biophys. J.* **1998**, *74*, 1871−1888.

(14) Itri, R.; Amaral, L. Q. Distance distribution function of sodium dodecyl-sulfate micelles by X-ray-scattering. *J. Phys. Chem.* **1991**, *95*, 423−427.

(15) Lauterwein, J.; Bosch, C.; Brown, L. R.; Wuthrich, K. Physicochemical studies of the protein-lipid interactions in melittin-containing micelles. *Biochim. Biophys. Acta* **1979**, *556*, 244−264.

(16) Wymore, T.; Gao, X. F.; Wong, T. C. Molecular dynamics simulation of the structure and dynamics of a dodecylphosphocholine micelle in aqueous solution. *J. Mol. Struct.* **1999**, *485*, 195−210.

(17) Jalili, S.; Akhavan, M. A coarse-grained molecular dynamics simulation of a sodium dodecyl sulfate micelle in aqueous solution. *Colloids Surf., A* **2009**, *352*, 99−102.

(18) Bruce, C. D.; Berkowitz, M. L.; Perera, L.; Forbes, M. D. E. Molecular dynamics simulation of sodium dodecyl sulfate micelle in water: Micellar structural characteristics and counterion distribution. *J. Phys. Chem. B* **2002**, *106*, 3788−3793.

(19) Gao, J.; Ge, W.; Hu, G. H.; Li, J. H. From homogeneous dispersion to micelles - A molecular dynamics simulation on the compromise of the hydrophilic and hydrophobic effects of sodium dodecyl sulfate in aqueous solution. *Langmuir* **2005**, *21*, 5223−5229.

(20) Bendedouch, D.; Chen, S. H.; Koehler, W. C. Structure of ionic micelles from small-angle neutron-scattering. *J. Phys. Chem.* **1983**, *87*, 153−159.

(21) Jones, R. R. M.; Maldonado, R.; Szajdzinskapietek, E.; Kevan, L. Electron-spin echo modulation of doxylstearic acid probes of the surface and internal structure of lithium dodecyl-sulfate micelles - comparison with sodium dodecyl-sulfate and tetramethylammonium dodecyl-sulfate micelles. *J. Phys. Chem.* **1986**, *90*, 1126−1129.

(22) Morrow, B. H.; Koenig, P. H.; Shen, J. K. Atomistic simulations of pH-dependent self-assembly of micelle and bilayer from fatty acids. *J. Chem. Phys.* **2012**, *137*.

(23) Jo, S.; Kim, T.; Im, W. Automated builder and database of protein/membrane complexes for molecular dynamics simulations. *PLoS One* **2007**, *2*.

(24) Jo, S.; Lim, J. B.; Klauda, J. B.; Im, W. CHARMM-GUI membrane builder for mixed bilayers and its application to yeast membranes. *Biophys. J.* **2009**, *97*, 50−58.

(25) Jo, S.; Kim, T.; Iyer, V. G.; Im, W. CHARMM-GUI: a Web-based graphical user interface for CHARMM. *J. Comput. Chem.* **2008**, *29*, 1859−1865.

(26) Miller, B. T.; Singh, R. P.; Klauda, J. B.; Hodoscek, M.; Brooks, B. R.; Woodcock, H. L., 3rd CHARMMing: a new, flexible Web portal for CHARMM. *J. Chem. Inf. Model.* **2008**, *48*, 1920−1929.

(27) Schmidt, T. H.; Kandt, C. LAMBADA and InflateGRO2: Efficient membrane alignment and insertion of membrane proteins for molecular dynamics simulations. *J. Chem. Inf. Model.* **2012**, *52*, 2657−2669.

(28) Park, S. H.; Marassi, F. M.; Black, D.; Opella, S. J. Structure and dynamics of the membrane-bound form of Pf1 coat protein: Implications of structural rearrangement for virus assembly. *Biophys. J.* **2010**, *99*, 1465−1474.

(29) Jo, S.; Kim, T.; Im, W. Automated builder and database of protein/membrane complexes for molecular dynamics simulations. *PLoS One* **2007**, *2*, e880.
(30) Jo, S.; Lim, J. B.; Klauda, J. B.; Im, W. CHARMM-GUI membrane builder for mixed bilayers and its application to yeast membranes. *Biophys. J.* **2009**, *97*, 50−58.
(31) Berman, H. M.; Westbrook, J.; Feng, Z.; Gilliland, G.; Bhat, T. N.; Weissig, H.; Shindyalov, I. N.; Bourne, P. E. The Protein Data Bank. *Nucleic Acids Res.* **2000**, *28*, 235−242.
(32) Lomize, M. A.; Lomize, A. L.; Pogozheva, I. D.; Mosberg, H. I. OPM: orientations of proteins in membranes database. *Bioinformatics* **2006**, *22*, 623−625.
(33) Berman, H. M.; Battistuz, T.; Bhat, T. N.; Bluhm, W. F.; Bourne, P. E.; Burkhardt, K.; Feng, Z.; Gilliland, G. L.; Iype, L.; Jain, S.; Fagan, P.; Marvin, J.; Padilla, D.; Ravichandran, V.; Schneider, B.; Thanki, N.; Weissig, H.; Westbrook, J. D.; Zardecki, C. The Protein Data Bank. *Acta Crystallogr., Sect. D: Biol. Crystallogr.* **2002**, *58*, 899−907.
(34) Brooks, B. R.; Brooks, C. L., III.; Mackerell, A. D., Jr.; Nilsson, L.; Petrella, R. J.; Roux, B.; Won, Y.; Archontis, G.; Bartels, C.; Boresch, S.; Caflisch, A.; Caves, L.; Cui, Q.; Dinner, A. R.; Feig, M.; Fischer, S.; Gao, J.; Hodoscek, M.; Im, W.; Kuczera, K.; Lazaridis, T.; Ma, J.; Ovchinnikov, V.; Paci, E.; Pastor, R. W.; Post, C. B.; Pu, J. Z.; Schaefer, M.; Tidor, B.; Venable, R. M.; Woodcock, H. L.; Wu, X.; Yang, W.; York, D. M.; Karplus, M. CHARMM: the biomolecular simulation program. *J. Comput. Chem.* **2009**, *30*, 1545−1614.
(35) Phillips, J. C.; Braun, R.; Wang, W.; Gumbart, J.; Tajkhorshid, E.; Villa, E.; Chipot, C.; Skeel, R. D.; Kale, L.; Schulten, K. Scalable molecular dynamics with NAMD. *J. Comput. Chem.* **2005**, *26*, 1781−1802.
(36) Klauda, J. B.; Venable, R. M.; Freites, J. A.; O'Connor, J. W.; Tobias, D. J.; Mondragon-Ramirez, C.; Vorobyov, I.; MacKerell, A. D.; Pastor, R. W. Update of the CHARMM all-atom additive force field for lipids: validation on six lipid types. *J. Phys. Chem. B* **2010**, *114*, 7830−7843.
(37) Jorgensen, W. L.; Chandrasekhar, J.; Madura, J. D.; Impey, R. W.; Klein, M. L. Comparison of simple potential functions for simulating liquid water. *J. Chem. Phys.* **1983**, *79*, 926−935.
(38) Feller, S. E.; Zhang, Y. H.; Pastor, R. W. Computer-simulation of liquid/liquid interfaces. 2. Surface-tension area dependence of a bilayer and monolayer. *J. Chem. Phys.* **1995**, *103*, 10267−10276.
(39) MacKerell, A. D.; Bashford, D.; Bellott, M.; Dunbrack, R. L.; Evanseck, J. D.; Field, M. J.; Fischer, S.; Gao, J.; Guo, H.; Ha, S.; Joseph-McCarthy, D.; Kuchnir, L.; Kuczera, K.; Lau, F. T. K.; Mattos, C.; Michnick, S.; Ngo, T.; Nguyen, D. T.; Prodhom, B.; Reiher, W. E.; Roux, B.; Schlenkrich, M.; Smith, J. C.; Stote, R.; Straub, J.; Watanabe, M.; Wiorkiewicz-Kuczera, J.; Yin, D.; Karplus, M. All-atom empirical potential for molecular modeling and dynamics studies of proteins. *J. Phys. Chem. B* **1998**, *102*, 3586−3616.
(40) Essmann, U.; Perera, L.; Berkowitz, M. L.; Darden, T.; Lee, H.; Pedersen, L. G. A smooth particle mesh Ewald method. *J. Chem. Phys.* **1995**, *103*, 8577−8593.
(41) Steinbach, P. J.; Brooks, B. R. New spherical-cutoff methods for long-range forces in macromolecular simulation. *J. Comput. Chem.* **1994**, *15*, 667−683.
(42) Lipfert, J.; Columbus, L.; Chu, V. B.; Lesley, S. A.; Doniach, S. Size and shape of detergent micelles determined by small-angle x-ray scattering. *J. Phys. Chem. B* **2007**, *111*, 12427−12438.
(43) MacKenzie, K. R.; Prestegard, J. H.; Engelman, D. M. A transmembrane helix dimer: structure and implications. *Science* **1997**, *276*, 131−133.
(44) Call, M. E.; Wucherpfennig, K. W.; Chou, J. J. The structural basis for intramembrane assembly of an activating immunoreceptor complex. *Nat. Immunol.* **2010**, *11*, 1023−U1073.
(45) Zhou, Y.; MacKinnon, R. The occupancy of ions in the K+ selectivity filter: charge balance and coupling of ion binding to a protein conformational change underlie high conduction rates. *J. Mol. Biol.* **2003**, *333*, 965−975.
(46) Pautsch, A.; Schulz, G. E. Structure of the outer membrane protein A transmembrane domain. *Nat. Struct. Biol.* **1998**, *5*, 1013−1017.
(47) Efremov, R. G.; Sazanov, L. A. Structure of Escherichia coli OmpF porin from lipidic mesophase. *J. Struct. Biol.* **2012**, *178*, 311−318.
(48) Cheng, X.; Im, W. NMR observable-based structure refinement of DAP12-NKG2C activating immunoreceptor complex in explicit membranes. *Biophys. J.* **2012**, *102*, L27−29.
(49) Cheng, X.; Jo, S.; Marassi, F. M.; Im, W. NMR-based simulation studies of pf1 coat protein in explicit membranes. *Biophys. J.* **2013**, *105*, 691−698.

NOTE ADDED AFTER ASAP PUBLICATION

This paper was published ASAP on August 5, 2013, with an incorrect version of Figure 3. The corrected version was published ASAP on August 7, 2013.